ACS NANO
Cite This: ACS Nano 2018, 12, 5913–5922
www.acsnano.org

ARTICLE

Metallic Nanoislands on Graphene for Monitoring Swallowing Activity in Head and Neck Cancer Patients

Julian Ramírez,[†] Daniel Rodriquez,[†] Fang Qiao,[‡] Julian Warchall,[§] Jasmine Rye,[†] Eden Aklile,[†] Andrew S.-C. Chiang,[†] Brandon C. Marin,[†] Patrick P. Mercier,[§] C. K. Cheng,[‡] Katherine A. Hutcheson,[∥] Eileen H. Shinn,[⊥] and Darren J. Lipomi*[,†]

[†]Department of NanoEngineering, University of California, San Diego, 9500 Gilman Drive, Mail Code 0448, La Jolla, California 92093-0448, United States

[‡]Department of Computer Science and Engineering, University of California, San Diego, 9500 Gilman Drive, Mail Code 0404, La Jolla, California 92093-0404, United States

[§]Department of Electrical and Computer Engineering, University of California, San Diego, 9500 Gilman Drive, Mail Code 0407, La Jolla, California 92093-0407, United States

[∥]Department of Head and Neck Surgery, The University of Texas MD Anderson Cancer Center, Unit 1445, 1515 Holcombe Street, Houston, Texas 77030-4009, United States

[⊥]Department of Behavioral Sciences, The University of Texas MD Anderson Cancer Center, Unit 1330, 1155 Pressler Street, Houston, Texas 77230-1439, United States

Supporting Information

ABSTRACT: **There is a need to monitor patients with cancer of the head and neck postradiation therapy, as diminished swallowing activity can result in disuse atrophy and fibrosis of the swallowing muscles. This paper describes a flexible strain sensor comprising palladium nanoislands on single-layer graphene. These piezoresistive sensors were tested on 14 disease-free head and neck cancer patients with various levels of swallowing function: from nondysphagic to severely dysphagic. The patch-like devices detected differences in (1) the consistencies of food boluses when swallowed and (2) dysphagic and nondysphagic swallows. When surface electromyography (sEMG) is obtained simultaneously with strain data, it is also possible to differentiate swallowing *vs* nonswallowing events. The plots of resistance *vs* time are correlated to specific events recorded by video X-ray fluoroscopy. Finally, we developed a machine-learning algorithm to automate the identification of bolus type being swallowed by a healthy subject (86.4%. accuracy). The algorithm was also able to discriminate between swallows of the same bolus from either the healthy subject or a dysphagic patient (94.7% accuracy). Taken together, these results may lead to noninvasive and home-based systems for monitoring of swallowing function and improved quality of life.**

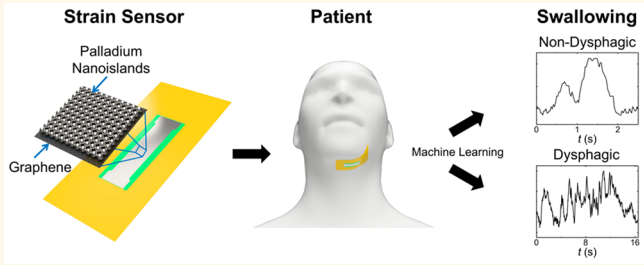

KEYWORDS: *graphene, nanoislands, wearable sensor, strain sensor, dysphagia, machine learning*

Multifunctional, wearable devices for health monitoring have the potential to reduce medical costs, increase patient comfort, and improve patient outcomes. These devices can do so by replacing or complementing invasive, painful, and costly diagnostic procedures with patchlike devices that can be applied by the patient at home. The consequences of sporadic, incomplete monitoring are especially severe following radiation therapy in patients with cancer of the head and neck.[1,2] In these patients, diminished swallowing activity and treatment effects lead to fibrosis, edema, disuse atrophy, and reduced function in swallowing. This paper describes a highly sensitive and flexible patchlike strain sensor that comprises palladium nanoislands on single-layer graphene. When attached to the skin in the submental region, below the chin, this piezoresistive sensor produces signals that indicate flexion of the swallowing muscles and passing of a bolus from the mouth to the esophagus. The objective of this work was to examine the hypothesis that these

Received: March 21, 2018
Accepted: June 6, 2018
Published: June 6, 2018

DOI: 10.1021/acsnano.8b02133
ACS Nano 2018, 12, 5913–5922

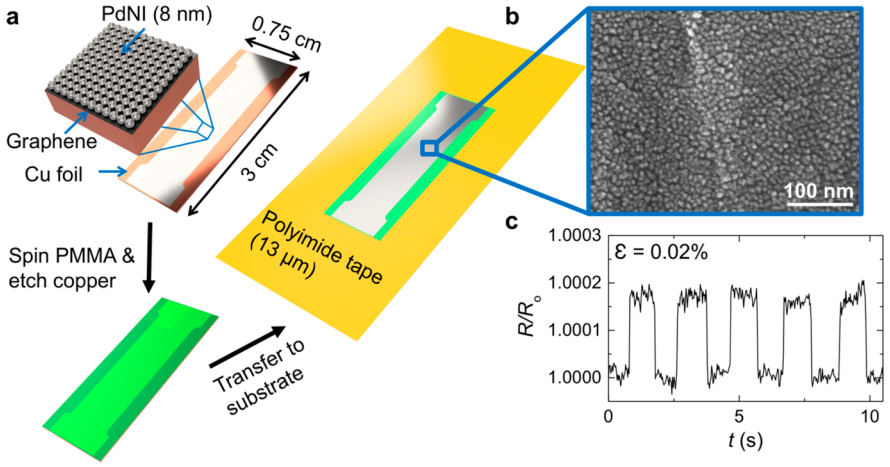

Figure 1. Schematic diagram depicting the fabrication of the palladium nanoisland (PdNI) strain sensor. (a) Fabrication process of the palladium nanoisland sensor on polyimide tape. (b) Scanning-electron microscope (SEM) image of the morphology of palladium nanoislands on a single layer of graphene. (c) Piezoresistive response of the composite film under a 0.02% strain that was determined by a cantilever strain experiment.

signals, combined with simultaneous readings from surface electromyography (sEMG), will allow detection of swallowing dysfunction, differentiation between swallowing and non-swallowing events, and differentiation of boluses of different consistencies by a machine-learning algorithm.

In 2017, 30360 new cases of laryngeal or pharyngeal cancers, and 6710 deaths from those diseases, were expected in the U.S.[3−6] Radiation therapy is commonly used for treatment, which can cause edema and eventually fibrosis (stiffening) of the swallowing musculature in up to 47% of head and neck cancer patients. These side effects of radiation contribute to the permanent development of moderate-to-severe dysphagia (abnormal or difficult swallowing) in up to 39% of head and neck cancer patients.[7] The ability to monitor the development of fibrotic tissue and deteriorating muscle function in cancer patients post-treatment is imperative to monitor the development of dysphagia. The most common method to monitor the development and severity of dysphagia is videofluoroscopy, commonly referred to as a modified barium swallow (MBS) exam. An MBS exam involves the video recording under continuous X-ray of a patient swallowing boluses of different consistencies.[8,9] Using videofluoroscopy, clinicians can grade the severity of dysphagia of a patient on a numerical scale (a grade of 1 corresponds to mild dysphagia and a grade of 4 corresponds to profound dysphagia).[10] While the MBS provides clinically useful data, it requires that the boluses be impregnated with barium to be detected and exposes patients to radiation. Furthermore, equipment for videofluoroscopy is expensive, requires trained personnel, and is only available in the clinic. Due to the limited access of speech pathologists trained in the treatment of head and neck cancer and the cost of gold-standard MBS tests, radiation-induced dysphagia is often diagnosed after there is little hope of restoring normal function.[11−15]

Techniques to measure physiological signals from the surface of the skin offer the potential for noninvasive monitoring without the need for visits to the clinic. sEMG monitors the electrical activity of a muscle when it is contracting. There are ongoing attempts to use sEMG to identify and monitor dysphagia in head and neck cancer patients, but such techniques have not been widely adopted because standard protocols were only recently established and because of the limitations of the type of data available to sEMG.[16−20] When used alone, sEMG is limited in the types of activities it can monitor. For example, sEMG monitors the electrical activity of muscles when they are actively contracting, but the relaxation of the swallowing muscles cannot be monitored. Continuous sensing of mechanical strain on the surface of the skin can, in principle, follow the contractions and relaxations of the submental muscles as a bolus is taken into the mouth and swallowed. Wearable sensors that use a piezoresistive mechanism are ubiquitous.[21] Researchers have used devices that consist of carbon-based nanomaterials,[22−25] as well as composite materials,[26−28] to detect subtle motions of the throat, such as respiration, speaking, and swallowing. Multiple groups have used various sensing modalities to assay swallowing activity.[29−34] However, these studies did not monitor the mechanical activity of muscle groups in the submental region, which are particularly susceptible to fibrosis following radiation therapy.[13] Here, we present a wearable piezoresistive sensor that comprises palladium nanoislands on single-layer graphene and its use in measuring the swallowing activity of head-and-neck cancer patients after radiotherapy. These palladium−graphene composites are used to detect swallowing activity by measuring the strain of the skin when a patient swallows a bolus. These sensors, when combined with conventional sEMG and a machine-learning algorithm, can be used to monitor patients in real time, while differentiating between signals that arise due to coughing, turning of the head, and swallowing of boluses of different consistencies.

RESULTS AND DISCUSSION

Characterization of Strain Sensor Device. As shown in Figure 1A, palladium nanoislands were deposited onto single-layer graphene by thermal evaporation using a stainless-steel mask to pattern the nanoislands into a dog-bone shape. The composite film was then transferred to a polyimide tape by a water transfer method (described in the Methods). The nanoscale morphology of 8 nm palladium on single-layer graphene supported by copper foil is depicted in Figure 1B. Morphologically, this palladium film consists of small islands that are separated by nanoscale gaps. The electrical resistance of the film is believed to be mediated in part by tunneling across these gaps, and thus, it is highly sensitive to mechanical

DOI: 10.1021/acsnano.8b02133
ACS Nano 2018, 12, 5913−5922

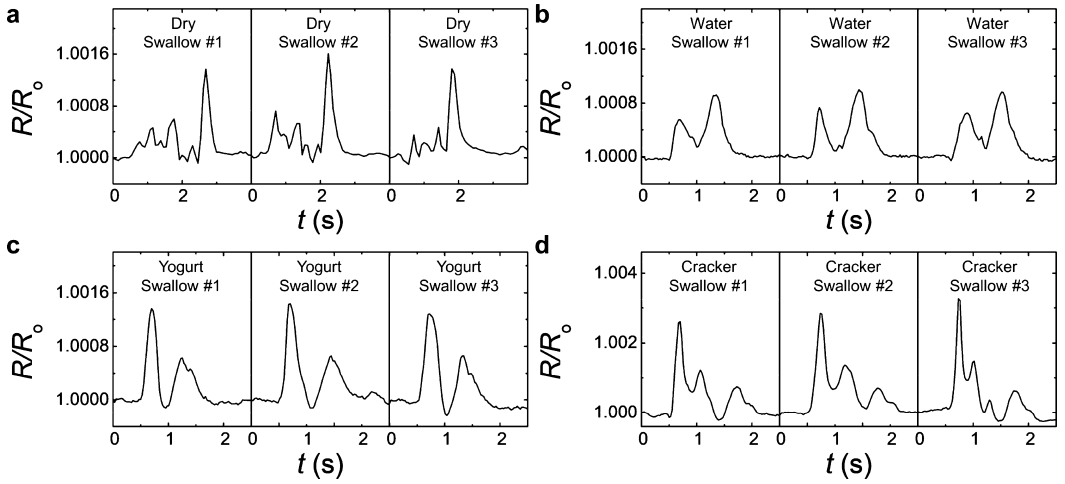

Figure 2. Signals (normalized resistance *vs* time) generated by the strain sensor as a healthy subject swallowed different boluses. (a) Signal of healthy subject performing a dry swallow. (b) Signal of the healthy subject swallowing a thin sip of water (~10 mL). (c) Signal of the healthy subject swallowing a tablespoon of yogurt (15 mL). (d) Signal of the healthy subject swallowing a masticated bite from a cracker.

strains.[35,36] Demonstrated in Figure 1C, the composite film had a piezoresistive response to a 0.02% bending strain and was able to reversibly detect this strain up to 115 cyclic bends (see Figure S1). A strain of 0.02% was chosen as it was similar to the strain the skin in the submental region experiences during swallowing. This approximation was determined by observing the change in the normalized resistance (R/R_0) to the bending strain and comparing it to the change in normalized resistance when a head and neck cancer patient (see Figure 3) swallowed 10 mL of water as a reference. The similar piezoresistive response to a patient swallowing a bolus and the bending strain confirm that our sensor on polyimide tape can easily detect strains that are physiologically relevant during swallowing.

On-Body Experiments: Healthy Subject. On-body experiments were performed with a healthy subject (age 24, male) prior to placing the sensors on head and neck cancer patients. As shown in Figure 2, swallows of different boluses resulted in distinctive and identifiable strain signals from the sensor. The signal from the patient performing a dry swallow can be seen in Figure 2A. The plot depicts multiple small events of tensile and compressive strain, followed by a brief instance of relaxation, and finished with a large tensile strain at the end of the swallow. On average, it took the healthy subject approximately 4 s to complete one dry swallow. The signal from the patient swallowing 10 mL of water is shown in Figure 2B. The swallowing signals contain two distinct tensile strain events, with the second being greater in magnitude than the first. The total time to complete the swallow of 10 mL of water was approximately 2 s. For the strain signal from the subject swallowing a tablespoon (15 mL) of yogurt, seen in Figure 2C, the first incidence of tensile strain was almost twice as large and narrower as the second tensile strain, and the swallow was performed in approximately 2 s. The signal from the subject swallowing a bite of a cracker, seen in Figure 2D, was similar to the signal from swallowing a tablespoon of yogurt, as the first instance in tensile strain was larger and narrower than the subsequent tensile strains. However, the tensile strains arising from the subject swallowing a cracker are greater in magnitude when compared to the signals of the subject swallowing a tablespoon of yogurt. Additionally, the time to perform the swallow for a cracker was longer than the time to swallow the yogurt bolus, and the signal from the subject swallowing a cracker contains a minor strain event, around 1 s, not observed in the signal from swallowing the yogurt. Further investigation demonstrated that the piezoresistive response of the device to swallowing events is not affected by an elevated heart rate in the human subject but can possibly be affected by the placement of the sensor with respect to the submental region (see Figures S2 and S3). The differences in the strain signals, namely strain magnitude and duration, allow for the identification of each bolus by visual observation.

On-Body Experiments: Head and Neck Cancer Patients. We further evaluated the practical utility of the palladium nanoisland sensors by detecting the flexion on the submental region of head and neck cancer patients with varying degrees of dysphagia during the ingestion of different bolus types. The placement of the strain sensor on the submental region of a patient and the signals from dysphagic and nondysphagic patients as they swallowed 10 mL of water are shown in parts A and B, respectively, of Figure 3. The degree of normalcy in the swallowing function of a nondysphagic patient can be evaluated by comparing the piezoresistive signal produced by the swallows of these patients to that produced by a healthy subject (age 24, male) (Figure 2). Two distinct increases in the resistance were observed due to the tensile strain experienced by the skin during a normal swallow. The first tensile strain event (Figure 3B, (i)) may reflect the contraction of submental muscles during the first phase of swallowing. Subsequently, the skin relaxed slightly, which caused the resistance to decrease before the second increase in resistance (Figure 3B, (ii)). This second peak is greater in magnitude than the first and may represent the larger strain experienced by the skin as the muscles contract to elevate the larynx and hyoid bone during the pharyngeal transit phase of the swallow. Completion of the swallowing process took approximately 2 s, as detected by the strain sensor, which was consistent with the completion time for the normal healthy subject. However, in dysphagic patients, the sensor detected strain signal patterns that were substantially different from the two distinct increases in normalized resistance detected for the nondysphagic patients. The sensor detected more than two events of tensile and compressive strain for dysphagic patients, which may reflect successive muscle contractions as they swallowed, as shown in the left column of Figure 3B.

DOI: 10.1021/acsnano.8b02133
ACS Nano 2018, 12, 5913−5922

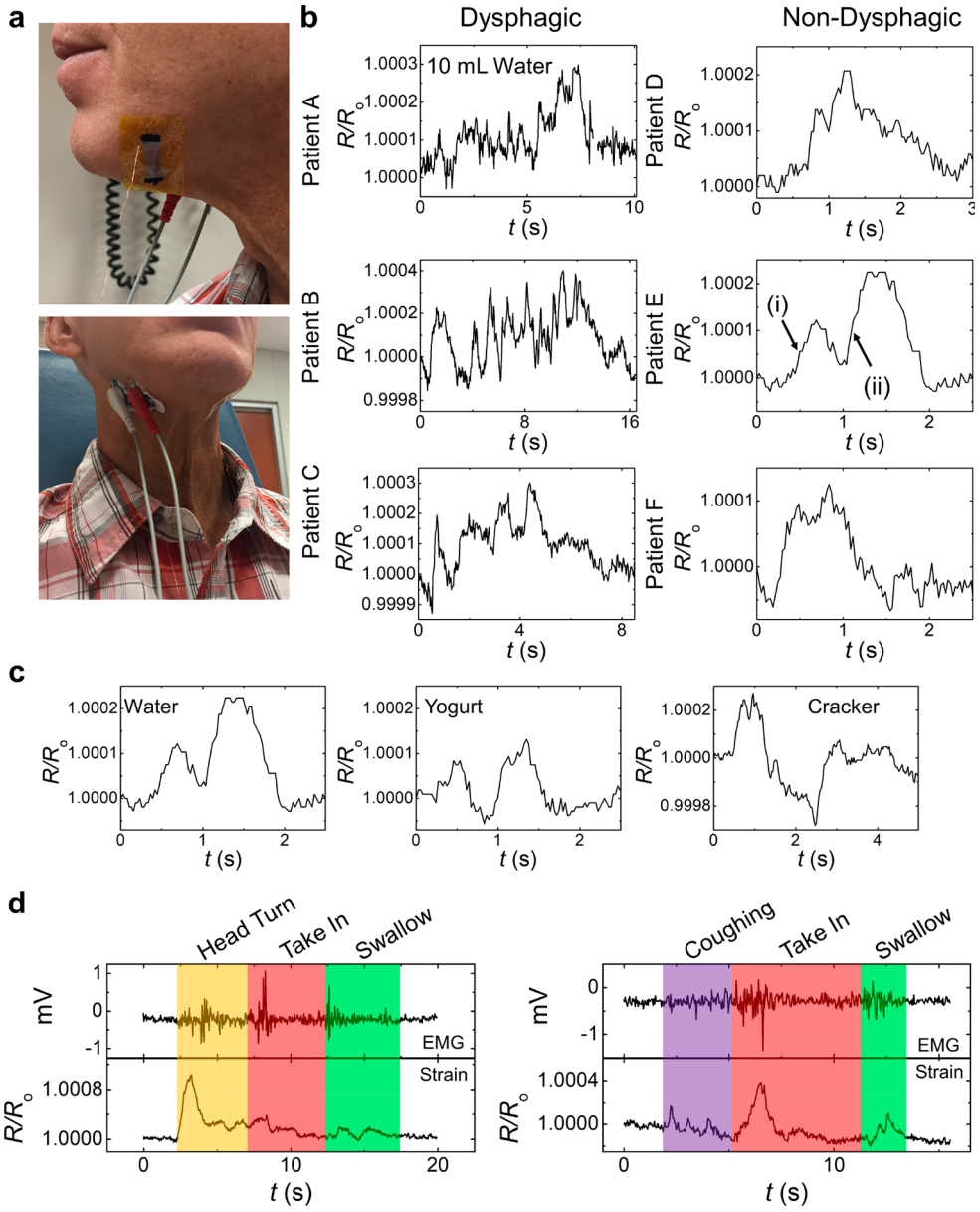

Figure 3. On-body experiments performed on dysphagic and nondysphagic patients. (a) Photographs depicting the palladium nanoisland sensor on single-layer graphene and sEMG sensor applied to the submental region of a dysphagic patient. (b) Signals from three dysphagic (left) and nondysphagic (right) patients while swallowing 10 mL of water. (c) Signals from a nondysphagic patient swallowing 10 mL of water, 15 mL of yogurt, and 6 g from a cracker. (d) Signals from a nondysphagic patient performing nonswallowing and swallowing activities.

Additionally, the total time for the dysphagic patient to swallow the bolus was significantly longer than for the nondysphagic patient. We observed a correlation between the amount of struggle and the severity of dysphagia a patient had when swallowing the bolus by examining the number of instances of tensile and compressive strain and the total time it took each patient to complete the swallow. Struggle manifests as unusually long times to swallow and many undulating features in the plots of resistance. We hypothesize that these characteristics may suggest the development of dysphagia.

The time and effort required to swallow a bolus also depends on bolus consistency, once chewed and mixed with saliva. The signals from the strain sensor for three different boluses (water, yogurt, and a cracker) from a single nondysphagic patient are shown in Figure 3C. The signals arising from swallowing these boluses were differentiated by (1) the magnitudes of tensile and compressive strains and (2) the timing and duration of these strain events. For the most fluid boluses (water and yogurt), the general shape of the curve and the time needed to complete the swallow were similar, but not identical. Small differences in the mechanical properties of these boluses (liquid *vs* viscoelastic liquid) affected the magnitudes of the strains measured at the surface of the skin. The consistency of the chewed cracker, however, was that of a thick paste, and the time needed by the patient to swallow the bolus increased. These observations of the properties of the boluses (*i.e.*, liquid *vs* paste) versus the time required to perform the swallow agree with previous studies for normal swallowing.[37]

Measurement of swallowing activity by strain alone can be confounded by motion artifacts (nonswallowing events). For example, coughs and head turns, which do not engage the swallowing muscles, may produce signals similar to those

DOI: 10.1021/acsnano.8b02133
ACS Nano 2018, 12, 5913−5922

produced by swallowing. In order to detect a swallowing event unambiguously, we measured strain and electrical activity simultaneously. The signals observed in both sensing modalities can offer further insight into the electrical stimuli and mechanical actuation of the muscles in the submental region during swallowing. The strain and sEMG signals of a nondysphagic patient as they turned their head from left to right (yellow) before facing forward and ingesting 10 mL of water (red and green) is shown in Figure 3D. By comparing the results from both the strain and sEMG sensors, we observed that the head turns from the nondysphagic patient produced only a small signal in the sEMG, but a large signal in the strain plot. Additionally, the movements stemming from the nondysphagic patient opening the mouth to take in the water, as well as swallowing the water, were clearly detectable by both the sEMG and the strain sensor. Another example of the identification of nonswallowing events using both sensing modalities can be seen in the adjacent plot, which depicts the signal of a strain sensor and sEMG sensor as the same nondysphagic patient coughed three times, sipped and held 10 mL of water, and finally swallowed the water. Similar to the signals observed when the patient turned their head, the three coughs performed by the patient produced a negligible signal by the sEMG sensor that was difficult to distinguish but produced three distinct strain signals detected by the strain sensor (Figure 3D, purple). While the coughs of the patient were not detected simultaneously by both the sEMG and strain-sensing modalities, the activity in the submental region as the patient took in 10 mL of water (Figure 3D, red) and swallowed the bolus (Figure 3D, green) was detected by both modalities. Because the strain sensor device detects larger strains for the nonswallowing events when compared to the swallowing events, the use of both sensing modalities can be useful in order to differentiate these nonswallowing artifacts from the swallowing events that clinicians are interested in. The bimodal plots also offer insight into muscle behavior, as the time for the strain sensor to relax was longer than that for the sEMG sensor. The difference in relaxation time suggests that the time it took for the electrical stimulus to actuate the muscle contraction to perform the swallow was shorter than the time it took for the muscles to perform the muscle contraction mechanically. The fact that the signal detected from the sEMG sensor was shorter in duration than the signal from the strain sensor may also be attributed to the time it took for the submental region to fully relax (*i.e.*, skin and biological tissue is viscoelastic).

The combination of the two sensing modalities can help speech pathologists gain more information about the swallowing function of a patient with respect to the electrical actuation of the muscles in the submental region and their mechanical performance. During the cohort study on head and neck cancer patients, we observed the quality of data acquired by these sensors may be reduced by the presence of loose skin and subcutaneous fat or edema. The elasticity of the skin in the submental region can be compromised due to many factors such as weight fluctuation, fibrosis, and the age of a patient. Furthermore, the formation of a dewlap on head and neck cancer patients, as a side effect, after radiation treatment can cause further separation of the skin surface from the swallowing muscles.[38] This separation can lessen the amount of strain and electrical signal detected on the surface of the skin due to the contraction of the muscles when swallowing.

Comparison of Strain Data to Videofluoroscopy. A device meant for home use is only valuable to the extent that the data collected by it matches data produced by procedures used in the clinic. We thus sought to assign features in the data obtained from the sensors to actual events occurring in the mouth and pharynx. In order to correlate the swallowing function recorded by the wearable sensors to actual swallowing activity, we compared the data to images of swallowing events obtained by videofluoroscopy performed after radiation therapy but not simultaneously acquired with sensor experiments due to the impracticality of obtaining these data concurrently. The strain signals of a dysphagic and nondysphagic patient with snapshots of their respective videofluoroscopy data overlaid at the appropriate time points is shown in Figure 4. By monitoring

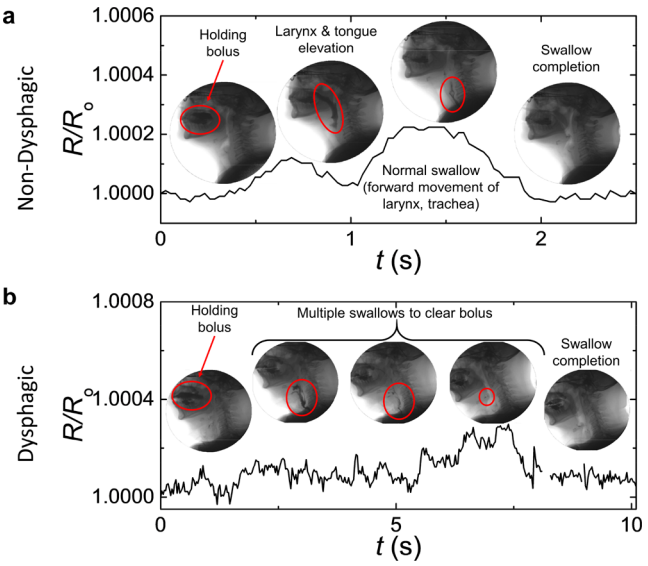

Figure 4. Correlation of strain data obtained from head and neck cancer patients with their corresponding videofluoroscopy experiments. The strain signals of (a) a nondysphagic patient (patient E) and (b) a dysphagic patient (patient A) when swallowing 10 mL of water were compared to videofluoroscopy experiments done on the patients at a previous time. Analysis of the videofluoroscopy experiments combined with strain signals indicate differences in the strain events and time to complete a swallow between the two patients. These differences are caused by the altered swallowing function of the dysphagic patient, for whom swallowing 10 mL of water required multiple swallows.

the strain signal of the nondysphagic patient and comparing it to the snapshots from the videofluoroscopy of the patient while swallowing a liquid barium solution of similar volume, we observed that the two distinct instances of tensile strain experienced on the skin may be attributed to the normal contractions of the muscles during a regular swallowing event (Figure 4A).[39,40] The first (smaller) strain event detected by the sensor appears attributed to the oral transit phase of the swallow, where the tongue propels the bolus to the back of the mouth and toward the pharynx. The second and larger tensile strain appears attributed to the pharyngeal phase of the swallow, which involves the contraction of the mylohyoid, digastric, and geniohyoid muscles as well as longitudinal pharyngeal muscles to protect the airway as the bolus moves toward the esophagus.[41−43] Conversely, the signal from the dysphagic patient differs significantly from the signal of the nondysphagic patient with respect to the duration of the

DOI: 10.1021/acsnano.8b02133
ACS Nano 2018, 12, 5913−5922

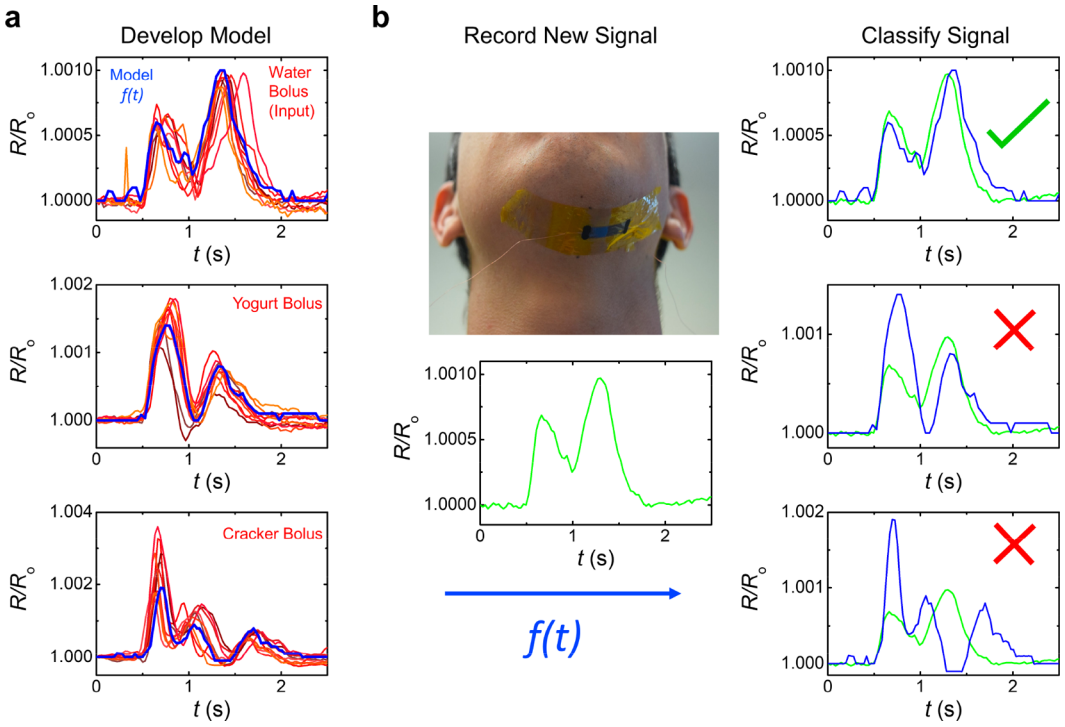

Figure 5. Schematic demonstrating the development and testing of the classification machine-learning algorithm using the bolus identification task as an example. The machine-learning algorithm was (a) first trained on the strain data of three boluses (red). Once the main features of the training data are extracted, a classifier algorithm (blue) was developed to (b) classify new swallowing data (green) into one of the three bolus categories. The accuracy of the model was assessed to be 86.4% by cross-validation techniques (see the Supporting Information). For details on model development and additional tasks performed, refer to the Supporting Information.

swallow and number of events where the skin in the submental region undergoes tensile and compressive strain (Figure 4B). By observing the videofluoroscopy results for this patient for a bolus similar to the one used during the strain measurements, the multiple peaks during the swallow and the longer time to complete the swallow might be attributed to the multiple swallows performed by the patient to ingest the bolus completely. Similar studies made by previous groups have determined that the swallowing complications of dysphagic patients will require them to ingest a single bolus by multiple successive swallows. The successive swallows arising from these complications will increase the duration to swallow a given bolus when compared to a nondysphagic patient.

Development of Machine-Learning Algorithm. Building upon visual analysis of the swallowing signals from on-body trials, we developed a machine-learning algorithm to perform preliminary tasks in order to differentiate swallowing signals as a proof-of-concept. The machine-learning algorithm was developed to automate identification tasks for multiple swallowing signals, either from a healthy subject (age 24, male) or a dysphagic patient, to perform two classification tasks. The first task of the machine-learning algorithm involved identifying a given swallowing signal from the healthy subject as the signal of the subject swallowing either 10 mL of water, 15 mL of yogurt, or 6 g of a cracker. The first task has relevance when considering that speech pathologists use food groups of different consistencies in order to make a more complete assessment of a patient's swallowing function. A schematic diagram of the development of the machine-learning algorithm, with the task of identifying a bolus used as an example is shown in Figure 5. Shown in Figure 5A, the algorithm was trained with multiple swallows of the three boluses (red gradient) to develop the classifier models for each signal (blue). Before developing the classifier models, the signals were preprocessed by interpolating the data to have regular time intervals per resistance measurement and by fitting an approximate smooth curve to minimize the amount of noise among signals of the same bolus (see Figure S4). The signals were then aligned with respect to time, and the features of the bolus signals were extracted by unsupervised learning (see Figure S5). After the extraction of the features, the three classifier models were developed to perform the bolus classification task, where the accuracy of the bolus identification algorithm was tested through cross-validation techniques. Figure 5B depicts a scenario in which a new swallowing signal (green) is identified as the signal of one of three boluses using the three classifier models as scoring metrics for identification. An efficient classification model based on the L1-distance of the per-class average (seen in eq S1) was the most accurate model, with an accuracy of 86.4% for the first task.

The second task involved identifying an unknown swallow (10 mL water) as either that of the healthy subject (age 24, male) or a patient exhibiting mild dysphagia (patient H in Table S1). The signals generated by the mildly dysphagic patient were similar to the signals generated by the healthy subject with respect to time scale and magnitude of strain, and thus, we presented an intentional challenge to the machine-learning algorithm. This task was designed to demonstrate whether or not the algorithm could detect cases of gradual deterioration in swallowing function on the way to dysphagia. This task, which used the data of a patient with mild dysphagia, mimics the creeping development of dysphagia more so than would comparing a healthy subject and a severely dysphagic patient. Given the ideal application for this device as a daily

DOI: 10.1021/acsnano.8b02133
ACS Nano 2018, 12, 5913−5922

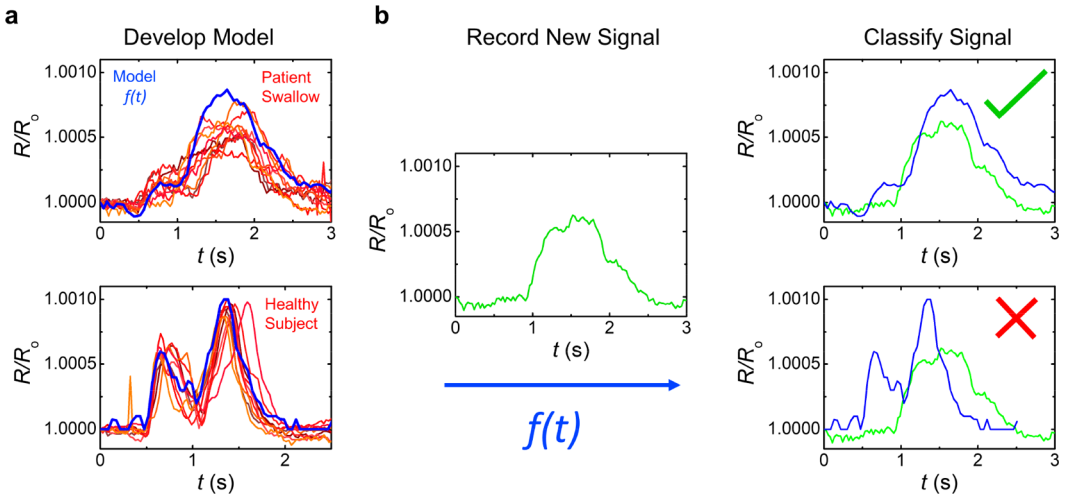

Figure 6. Schematic demonstrating the development and testing of the classification machine-learning algorithm using the bolus identification task as an example. The machine-learning algorithm (a) was first trained on the strain data of both human subjects (red). Once the main features of the training data are extracted, a classifier algorithm (blue) was developed to (b) classify new swallowing data (green) as either the swallowing of 10 mL by a healthy subject or a dysphagic patient. The accuracy of the model was assessed to be 94.7% by cross-validation techniques (see the Supporting Information). Details on the model development and additional tasks performed can be seen in the Supporting Information.

complement to the MBS exam, which can only be administered periodically (one exam every 3−6 months), the device paired with the machine-learning algorithm would have to detect the gradual evolution in swallowing activity over time. As shown in Figure 6A, the algorithm was trained with multiple swallows of either the healthy subject or the dysphagic patient (red gradients) to develop the classifier models for each situation (blue). After the extraction of the features, the two classifier models were developed to perform the subject classification task, where the accuracy of the algorithm was tested through cross-validation techniques. Figure 6B depicts a scenario in which a new swallowing signal (green) is identified as either the swallow of a healthy subject or the swallow of a dysphagic patient, using the classifier models as scoring metrics for identification. Similar to the first task, the classification model based on the L1-distance of the per-class average was the most accurate model, with an accuracy of 94.7%. The tasks performed by the machine-learning algorithm demonstrate the potential to combine algorithms with wearable sensors to monitor and potentially identify degradation in the swallowing function of head and neck cancer patients. Moreover, the use of machine-learning algorithms which combine input from both strain and sEMG measurements could potentially be used to differentiate degradation in swallowing activity arising from radiation therapy from degradation arising from other diseases of the head and neck.

CONCLUSIONS

The wearable and flexible strain sensor presented here demonstrates the potential for remote monitoring of patients outside of the clinic. Its distinctive morphology, resulting from the growth of palladium nanoparticles on graphene, produces a piezoresistive response sufficiently sensitive for detecting strains of physiological importance. By exploiting the exceptional piezoresistive properties, we fabricated a device capable of detecting swallowing activity for the remote monitoring of dysphagia. The real-world utility of this device was investigated by recording the swallowing activity of 14 head and neck cancer patients when placed on the submental region. The strain sensor was able to detect differences in swallowing activity based on (1) the type of boluses being ingested by a healthy noncancer subject and a nondysphagic patient and (2) functional *vs* dysphagic swallow status in head and neck cancer patients who had been treated with radiation to the throat. Combining the piezoresistive sensing modality with sEMG also provided further insight as to how the muscles in the submental region are actuated and how they relax after swallowing. Comparison of these noninvasive methods with videofluoroscopy—the current gold standard, in which a paste containing barium is swallowed under X-ray irradiation—suggests that our patch-like devices have the potential to produce data of sufficient clinical value to permit self-monitoring, and ultimately increase the quality of life of head and neck cancer survivors. A proof-of-concept machine-learning algorithm was developed to identify the bolus being swallowed by a healthy subject and to distinguish between the signals of a healthy subject and a dysphagic patient swallowing the same bolus, highlighting further potential use of wearable devices by clinicians.

METHODS

Wearable Palladium Nanoisland Sensor. Single-layer graphene, supported on a copper foil substrate, was purchased from Graphenea. A nominal thickness of 8 nm of palladium nanoislands was deposited on top of the graphene on copper foil using thermal evaporation on an Orion System (AJA International) at a rate of 0.02 Å/s. A stainless steel stencil (Metal Etch Services, San Marcos, CA) was used to deposit the palladium nanoislands in a dog bone shape, as shown in Figure 1. 50 nm of aluminum was deposited at 1.5 Å/s on top of the palladium by sputtering. The aluminum layer served as a mask to selectively etch off the graphene around the dog bone pattern. The graphene surrounding the dog bone was then etched by oxygen plasma for 5 min. Afterward, the graphene on the back of the copper foil was etched off by oxygen plasma for 5 min. Similarly, the aluminum film was etched by submerging the sensor films into 0.025 M KOH in water (Fisher Scientific) for 1 min, leaving the dog bone shape that comprises palladium nanoislands on a single layer of graphene. After etching the aluminum film, 4% PMMA (by mass) (Alfa Aesar) in anisole (Acros Organics) was deposited on top of the palladium nanoislands/graphene/copper by spin coating (4000 rpm, 4000 rpm/s, 60 s). The film was then heated to 150 °C for 10 min to remove

DOI: 10.1021/acsnano.8b02133
ACS Nano 2018, 12, 5913−5922

residual solvent. The supporting copper foil was etched away in 0.05 g/mL ammonium persulfate (Acros Organics) in water. The film of PMMA/palladium nanoislands/graphene was transferred out of the ammonium persulfate by adhering the edge of the film to a glass slide, lifting out the film from the ammonium persulfate, and plunging the glass slide into a water bath, releasing the film on the surface of the water. The PMMA/palladium nanoislands/graphene film was then transferred onto the final receiving substrate (Caplinq, Product No. PIT0.5S UT/25.4) by adhering one edge of the film onto the polyimide tape, supported on a glass slide, and plunging the glass slide into the water bath. The transfer results in the PMMA film being adhered to the polyimide tape, with the graphene facing upward (graphene/palladium nanoislands/PMMA/polyimide tape). The substrate used to develop the strain sensor for this study—a polyimide tape that is 13 μm thick—offered mechanical robustness and flexibility sufficient to accommodate mechanical deformations of the submental region during swallowing. The sensor was then addressed with copper wire, with a carbon paint painted on the contact area (DAG-T-502, Ted Pella, Inc.) and left to dry.

Cantilever Strain Experiment. For the cantilever strain experiment, the device was adhered to a 1 × 2 in willow glass substrate (Corning) as a cantilever substrate. The device on willow glass was then partially suspended, clamped at a 1 cm overlap, over a step edge of a 1.25 mm using Si wafers (University Wafer), with the strain sensor fully suspended in air. The tensile strain applied to the sensor device was calculated using a simple continuum mechanics model.[44] The axial strain is modeled analytically by the equation

$$\varepsilon_{ZZ} = \frac{6bh}{4L^2 - 5aL + a^2}$$

where b is the step edge height, h is the thickness of the substrate, a is the distance from the clamped end to the nanowire, and L is the total length between clamped end and displaced end. By the dimensions of our experimental setup on AutoCAD, we determined the strain experienced by the device during the cantilever experiment corresponds to a radius of curvature of approximately 58 cm.

Strain and sEMG Sensor Placement and Data Acquisition. Before placing the wearable strain sensor on the submental region of the healthy human subject or head and neck cancer patients, the area of interest was wiped with 2-propanol to remove oil and dirt from the skin. A makeup adhesive (Spirit Gum, Mehron) was brushed onto the adhesive side of the tape of the sensor substrate. The makeup adhesive was left to dry for approximately 5 min before the sensor was placed onto the skin. The sensor was placed on the surface of the skin in the submental region, where the mylohyoid and geniohyoid muscles are. Conventional sEMG electrodes were used in parallel with the strain sensor. In clinical practice using sEMG biofeedback for therapeutic applications with dysphagic populations, the most common placements are in the submental region and lateral to the larynx. For the sEMG sensing modality, the reference electrode was placed on the skin surface near the carpal bone of the left wrist. The working and counter electrodes were placed on the surface of the skin in the submental region, symmetrically across from the strain sensor and atop the same muscle groups next to where the strain sensor was placed. The sEMG circuit was configured to use a low-pass filter of 2 kHz and a high-pass filter of 30 Hz. The signal was amplified with a minimum gain of 550 and a max gain of 1600. sEMG Red Dot electrodes were purchased from 3 M (Model 2560) and used as received. The strain sensor device was addressed to a Keithley 2601B SourceMeter to acquire the strain sensor data and the sEMG data was acquired by a Keithley 2400 SourceMeter. Both the strain and sEMG data was sent to LabVIEW for recording and processing.

On-Body Experiments on Head and Neck Cancer Patients. On-body tests were first performed on a completely healthy subject (age 24, male) before being conducted on 14 head and neck cancer patients who were previously treated with radiation therapy. This study consisted of 12 male and two female patients of ages ranging from 43 to 83 years. Seven out of these 14 patients were diagnosed based on videofluoroscopy with at least moderate dysphagia (DIGEST grade ≥2). In six out of the seven dysphagic cases, DIGEST scores (grade ≥2) were commensurate with self-reported status. In the seventh case, a recent MBS was not available but patient's dysphagic status was verified with physician observation, based on long-term gastrostomy dependence with poor secretion management. All seven patients who suffered from dysphagia underwent radiation therapy to bilateral cervical fields. All on-body experiments on head and neck cancer patients were performed with approval from an Internal Review Board (Protocol No. 2016-0597) of MD Anderson Cancer Center. For the swallowing experiments, the boluses consisted of a small sip of water (10 mL), a tablespoon (15 mL) of yogurt, or a bite from a cracker (~6 g). The healthy subject and patients were asked to take in a bolus into their mouth, hold the bolus in their mouth until the signals from the strain sensor baselined, and then were asked to swallow the bolus.

Machine-Learning Analysis. Machine-learning algorithms have recently been implemented in applications that involve interpreting and analyzing sensor data.[45,46] We developed a machine-learning algorithm around our strain sensor data to determine if statistical models could correctly classify new swallowing signals. First, we established whether or not swallowing signals for a given subject could be classified based on the bolus being swallowed (liquid, yogurt, or cracker). Second, we determined if the swallowing signal of a healthy subject (age 24, male) could be distinguished from that of a dysphagic one (DIGEST grade 4). Performing tasks such as identifying boluses being swallowed by a patient and identifying abnormal swallowing could offer swallowing information, usually acquired in a clinic, to a speech pathologist remotely and without the need to limit the diet of a patient. Wearable systems that can obtain and analyze data could help clinicians monitor the development of dysphagia in head and neck cancer patients and potentially obtain a much earlier diagnosis than is possible using current methods.

ASSOCIATED CONTENT

Supporting Information

The Supporting Information is available free of charge on the ACS Publications website at DOI: 10.1021/acsnano.8b02133.

Patients' medical information as well as figures, tables, and equations detailing the methods used for the proof-of-concept machine-learning tasks (PDF)

AUTHOR INFORMATION

Corresponding Author

*E-mail: dlipomi@eng.ucsd.edu.

ORCID

Patrick P. Mercier: 0000-0003-1488-5076

Darren J. Lipomi: 0000-0002-5808-7765

Notes

The authors declare no competing financial interest.

ACKNOWLEDGMENTS

This work was supported by the National Institutes of Health Director's New Innovator Award, Grant No. 1DP2EB022358-01 to D.J.L. and by a Diversity Supplement (for B.C.M.) under Award No. 1DP2EB022358-01S1. E.A. received partial support from the CANASA/UCSD Space Grant Consortium. J.R. and D.R. acknowledge support provided by the National Science Foundation Graduate Research Fellowship Program under Grant No. DGE-1144086. This work was performed in part at the San Diego Nanotechnology Infrastructure (SDNI), a member of the National Nanotechnology Coordinated Infrastructure, which is supported by the National Science Foundation (Grant No. ECCS-1542148). This work was performed in part at the University of Texas MD Anderson Cancer center, which is supported by the NCI Cancer Center

DOI: 10.1021/acsnano.8b02133
ACS Nano 2018, 12, 5913−5922

Support Grant (P30CA016672). We also thank Mohammad A. Alkhadra for his help in proofreading the manuscript.

REFERENCES

(1) Rosenthal, D. I.; Lewin, J. S.; Eisbruch, A. Prevention and Treatment of Dysphagia and Aspiration after Chemoradiation for Head and Neck Cancer. *J. Clin. Oncol.* **2006**, *24*, 2636−2643.

(2) Bleier, B. S.; Levine, M. S.; Mick, R.; Rubesin, S. E.; Sack, S. Z.; McKinney, K.; Mirza, N. Dysphagia after Chemoradiation: Analysis by Modified Barium Swallow. *Ann. Otol., Rhinol., Laryngol.* **2007**, *116*, 837−841.

(3) American Cancer Society. *Cancer Facts & Figures 2017*; American Cancer Society, 2017; p 1.

(4) Siegel, R. L.; Miller, K. D.; Jemal, A. Cancer Statistics, 2017. *Ca-Cancer J. Clin.* **2017**, *67*, 7−30.

(5) Howlader, N.; Noone, A. M.; Krapcho, M.; Neyman, N.; Aminou, R.; Altekruse, S. F.; Kosary, C. L.; Ruhl, J.; Tatalovich, Z.; Cho, H.; Mariotto, A.; Eisner, M. P.; Leiws, D. R.; Chen, H. S.; Feuer, E. J.; Cronin, K. A. *SEER Cancer Statistics Review, 1975−2009 (Vintage 2009 Populations)*; National Cancer Institute, 2011.

(6) Garden, A. S.; Kies, M. S.; Morrison, W. H.; Weber, R. S.; Frank, S. J.; Glisson, B. S.; Gunn, G. B.; Beadle, B. M.; Ang, K. K.; Rosenthal, D. I.; Sturgis, E. M. Outcomes and Patterns of Care of Patients with Locally Advanced Oropharyngeal Carcinoma Treated in the Early 21st Century. *Radiat. Oncol.* **2013**, *8*, 21.

(7) Ridner, S. H.; Dietrich, M. S.; Niermann, K.; Cmelak, A.; Mannion, K.; Murphy, B. A Prospective Study of the Lymphedema and Fibrosis Continuum in Patients with Head and Neck Cancer. *Lymphatic Res. Biol.* **2016**, *14*, 198−205.

(8) Logemann, J. A. Role of the Modified Barium Swallow in Management of Patients with Dysphagia. *Otolaryngol.–Head Neck Surg.* **1997**, *116*, 335−338.

(9) Martin-Harris, B.; Logemann, J. a.; McMahon, S.; Schleicher, M.; Sandidge, J. Clinical Utility of the Modified Barium Swallow. *Dysphagia* **2000**, *15*, 136−141.

(10) Hutcheson, K. A.; Barrow, M. P.; Barringer, D. A.; Knott, J. K.; Lin, H. Y.; Weber, R. S.; Fuller, C. D.; Lai, S. Y.; Alvarez, C. P.; Raut, J.; Lazarus, C. L.; May, A.; Patterson, J.; Roe, J. W.; Starmer, H. M.; Lewin, J. S. Dynamic Imaging Grade of Swallowing Toxicity (DIGEST): Scale Development and Validation. *Cancer* **2017**, *123*, 62−70.

(11) Mortensen, H. R.; Jensen, K.; Aksglæde, K.; Behrens, M.; Grau, C. Late Dysphagia after IMRT for Head and Neck Cancer and Correlation with Dose-Volume Parameters. *Radiother. Oncol.* **2013**, *107*, 288−294.

(12) Caudell, J. J.; Schaner, P. E.; Meredith, R. F.; Locher, J. L.; Nabell, L. M.; Carroll, W. R.; Magnuson, J. S.; Spencer, S. A.; Bonner, J. A. Factors Associated With Long-Term Dysphagia After Definitive Radiotherapy for Locally Advanced Head-and-Neck Cancer. *Int. J. Radiat. Oncol., Biol., Phys.* **2009**, *73*, 410−415.

(13) Dale, T.; Hutcheson, K.; Mohamed, A. S. R.; Lewin, J. S.; Gunn, G. B.; Rao, A. U. K.; Kalpathy-Cramer, J.; Frank, S. J.; Garden, A. S.; Messer, J. A.; Warren, B.; Lai, S. Y.; Beadle, B. M.; Morrison, W. H.; Phan, J.; Skinner, H.; Gross, N.; Ferrarotto, R.; Weber, R. S.; Rosenthal, D. I.; et al. Beyond Mean Pharyngeal Constrictor Dose for Beam Path Toxicity in Non-Target Swallowing Muscles: Dose-Volume Correlates of Chronic Radiation-Associated Dysphagia (RAD) after Oropharyngeal Intensity Modulated Radiotherapy. *Radiother. Oncol.* **2016**, *118*, 304−314.

(14) Caudell, J. J.; Schaner, P. E.; Desmond, R. A.; Meredith, R. F.; Spencer, S. A.; Bonner, J. A. Dosimetric Factors Associated With Long-Term Dysphagia After Definitive Radiotherapy for Squamous Cell Carcinoma of the Head and Neck. *Int. J. Radiat. Oncol., Biol., Phys.* **2010**, *76*, 403−409.

(15) Caglar, H. B.; Tishler, R. B.; Othus, M.; Burke, E.; Li, Y.; Goguen, L.; Wirth, L. J.; Haddad, R. I.; Norris, C. M.; Court, L. E.; Aninno, D. J.; Posner, M. R.; Allen, A. M. Dose to Larynx Predicts for Swallowing Complications After Intensity-Modulated Radiotherapy. *Int. J. Radiat. Oncol., Biol., Phys.* **2008**, *72*, 1110−1118.

(16) Gupta, V.; Reddy, N. P.; Canilang, E. P. Surface EMG Measurements at the Throat during Dry and Wet Swallowing. *Dysphagia* **1996**, *11*, 173−179.

(17) Vaiman, M.; Eviatar, E. Surface Electromyography as a Screening Method for Evaluation of Dysphagia and Odynophagia. *Head Face Med.* **2009**, *5*, 9.

(18) Vaiman, M. Standardization of Surface Electromyography Utilized to Evaluate Patients with Dysphagia. *Head Face Med.* **2007**, *3*, 26.

(19) Yoshida, M.; Groher, M. E.; Crary, M. A.; Mann, G. C.; Akagawa, Y. Comparison of Surface Electromyographic (sEMG) Activity of Submental Muscles between the Head Lift and Tongue Press Exercises as a Therapeutic Exercise for Pharyngeal Dysphagia. *Gerodontology* **2007**, *24*, 111−116.

(20) Constantinescu, G.; Jeong, J. W.; Li, X.; Scott, D. K.; Jang, K. I.; Chung, H. J.; Rogers, J. A.; Rieger, J. Epidermal Electronics for Electromyography: An Application to Swallowing Therapy. *Med. Eng. Phys.* **2016**, *38*, 807−812.

(21) Segev-Bar, M.; Haick, H. Flexible Sensors Based on Nanoparticles. *ACS Nano* **2013**, *7*, 8366−8378.

(22) Tao, L.-Q.; Wang, D.-Y.; Tian, H.; Ju, Z.-Y.; Liu, Y.; Pang, Y.; Chen, Y.-Q.; Yang, Y.; Ren, T.-L. Self-Adapted and Tunable Graphene Strain Sensors for Detecting Both Subtle and Large Human Motions. *Nanoscale* **2017**, *9*, 8266−8273.

(23) Tao, L.-Q.; Tian, H.; Liu, Y.; Ju, Z.-Y.; Pang, Y.; Chen, Y.-Q.; Wang, D.-Y.; Tian, X.-G.; Yan, J.-C.; Deng, N.-Q.; Yang, Y.; Ren, T.-L. An Intelligent Artificial Throat with Sound-Sensing Ability Based on Laser Induced Graphene. *Nat. Commun.* **2017**, *8*, 14579.

(24) Xu, R.; Wang, D.; Zhang, H.; Xie, N.; Lu, S.; Qu, K. Simultaneous Detection of Static and Dynamic Signals by a Flexible Sensor Based on 3D Graphene. *Sensors* **2017**, *17*, 1069.

(25) Wang, L.; Jackman, J. A.; Tan, E.; Park, J. H.; Potroz, M. G.; Hwang, E. T.; Cho, N.-J. High-Performance, Flexible Electronic Skin Sensor Incorporating Natural Microcapsule Actuators. *Nano Energy* **2017**, *36*, 38−45.

(26) Hwang, B. U.; Lee, J. H.; Trung, T. Q.; Roh, E.; Kim, D. Il; Kim, S. W.; Lee, N. E. Transparent Stretchable Self-Powered Patchable Sensor Platform with Ultrasensitive Recognition of Human Activities. *ACS Nano* **2015**, *9*, 8801−8810.

(27) Zhu, Y.; Hu, Y.; Zhu, P.; Zhao, T.; Liang, X.; Sun, R.; Wong, C. Enhanced Oxidation Resistance and Electrical Conductivity Copper Nanowires−graphene Hybrid Films for Flexible Strain Sensors. *New J. Chem.* **2017**, *41*, 4950−4958.

(28) Li, W.; Guo, J.; Fan, D. 3D Graphite-Polymer Flexible Strain Sensors with Ultrasensitivity and Durability for Real-Time Human Vital Sign Monitoring and Musical Instrument Education. *Adv. Mater. Technol.* **2017**, *2*, 1700070.

(29) Ertekin, C.; Pehlivan, M.; Aydoğdu, I.; Ertaşl, M.; Uludağ, B.; Çlelebi, G.; Çlolakoğlu, Z.; Sağduyu, A.; Yüceyar, N. An Electrophysiological Investigation of Deglutition in Man. *Muscle Nerve* **1995**, *18*, 1177−1186.

(30) Ertekin, C. Electrophysiological Evaluation of Oropharyngeal Swallowing in Myotonic Dystrophy. *J. Neurol., Neurosurg. Psychiatry* **2001**, *70*, 363−371.

(31) Ashida, I.; Miyaoka, S.; Miyaoka, Y. Comparison of Video-Recorded Laryngeal Movements during Swallowing by Normal Young Men with Piezoelectric Sensor and Electromyographic Signals. *J. Med. Eng. Technol.* **2009**, *33*, 496−501.

(32) Li, Q.; Hori, K.; Minagi, Y.; Ono, T.; Chen, Y.; Kondo, J.; Fujiwara, S.; Tamine, K.; Hayashi, H.; Inoue, M.; Maeda, Y. Development of a System to Monitor Laryngeal Movement during Swallowing Using a Bend Sensor. *PLoS One* **2013**, *8*, No. e70850.

(33) Schultheiss, C.; Schauer, T.; Nahrstaedt, H.; Seidl, R. O. Automated Detection and Evaluation of Swallowing Using a Combined Emg/bioimpedance Measurement System. *Sci. World J.* **2014**, *2014*, 1.

(34) Schultheiss, C.; Schauer, T.; Nahrstaedt, H.; Seidl, R. O. Evaluation of an EMG Bioimpedance Measurement System for

DOI: 10.1021/acsnano.8b02133
ACS Nano 2018, 12, 5913−5922

Recording and Analysing the Pharyngeal Phase of Swallowing. *Eur. Arch. Oto-Rhino-Laryngology* **2013**, *270*, 2149−2156.
(35) Zaretski, A. V.; Root, S. E.; Savchenko, A.; Molokanova, E.; Printz, A. D.; Jibril, L.; Arya, G.; Mercola, M.; Lipomi, D. J. Metallic Nanoislands on Graphene as Highly Sensitive Transducers of Mechanical, Biological, and Optical Signals. *Nano Lett.* **2016**, *16*, 1375−1380.
(36) Marin, B. C.; Ramirez, J.; Root, S. E.; Aklile, E.; Lipomi, D. J. Metallic Nanoislands on Graphene: A Metamaterial for Chemical, Mechanical, Optical, and Biological Applications. *Nanoscale Horiz.* **2017**, *2*, 311.
(37) Reimers-Neils, L.; Logemann, J.; Larson, C. Viscosity Effects on EMG Activity in Normal Swallow. *Dysphagia* **1994**, *9*, 101−106.
(38) Young, J. R. Radiation Dewlap. *Clin. Otolaryngol.* **1979**, *4*, 25−28.
(39) Standring, S. *Gray's Anatomy: The Anatomical Basis of Clinical Practice*, 41st ed.; 2016.
(40) Mankekar, G. *Swallowing - Physiology, Disorders, Diagnosis and Therapy*; Springer, 2015.
(41) Pearson, W. G.; Langmore, S. E.; Yu, L. B.; Zumwalt, A. C. Structural Analysis of Muscles Elevating the Hyolaryngeal Complex. *Dysphagia* **2012**, *27*, 445−451.
(42) Pearson, W. G.; Hindson, D. F.; Langmore, S. E.; Zumwalt, A. C. Evaluating Swallowing Muscles Essential for Hyolaryngeal Elevation by Using Muscle Functional Magnetic Resonance Imaging. *Int. J. Radiat. Oncol., Biol., Phys.* **2013**, *85*, 735−740.
(43) Shaw, S. M.; Martino, R. The Normal Swallow: Muscular and Neurophysiological Control. *Otolaryngol. Clin. North Am.* **2013**, *46*, 937−956.
(44) Jibril, L.; Ramírez, J.; Zaretski, A. V.; Lipomi, D. J. Single-Nanowire Strain Sensors Fabricated by Nanoskiving. *Sens. Actuators, A* **2017**, *263*, 702−706.
(45) Jeon, H.; Lee, W.; Park, H.; Lee, H.; Kim, S.; Kim, H.; Jeon, B.; Park, K. Automatic Classification of Tremor Severity in Parkinson's Disease Using a Wearable Device. *Sensors* **2017**, *17*, 2067.
(46) Lonini, L.; Shawen, N.; Ghaffari, R.; Rogers, J.; Jayarman, A. Automatic Detection of Spasticity from Flexible Wearable Sensors. In *Proceedings of the 2017 ACM International Joint Conference on Pervasive and Ubiquitous Computing and Proceedings of the 2017 ACM International Symposium on Wearable Computers on - UbiComp '17*; ACM Press: New York, 2017; pp 133−136.

DOI: 10.1021/acsnano.8b02133
ACS Nano 2018, 12, 5913−5922